

Diffusion-weighted imaging findings in brain death

Hakan Selcuk · Sait Albayram · Ercan Tureci ·
Zehra Isik Hasiloglu · Osman Kizilkilic · Emin Cagil ·
Naci Kocer · Civan Islak

Received: 31 March 2011 / Accepted: 6 July 2011 / Published online: 27 July 2011
© Springer-Verlag 2011

Abstract

Introduction The purpose of the present study was to determine the role of diffusion-weighted imaging (DWI) and to investigate the use of DWI in the diagnosis of brain death (BD).

Methods We prospectively evaluated 22 patients diagnosed with clinical BD (9 women, 13 men; mean age, 39.63 ± 15.1 years; age range, 9–66 years). All clinical criteria for BD were present in all 22 patients before magnetic resonance imaging, including a positive apnea test. For all cases, DW images, T2-weighted images, and fluid-attenuated inversion recovery were obtained. Thirteen distinct neuroanatomical structures were selected for analysis in all the cases. For each region of interest, the mean, standard deviation, and range of the average apparent diffusion coefficient (ADC_{av}) values were obtained.

Results For BD patients, ADC values in all neuroanatomical structures were significantly lower than those for control subjects. We determined how ADC values in all structures were related to the diagnostic condition as well as the appropriate threshold ADC values to classify a subject as BD

or control. The sensitivity, specificity, positive and negative predictive values, and correct classification rate of ADC cutoff values to distinguish BD from control groups were 100%.

Conclusions DWI might be used as a noninvasive confirmatory test for the diagnosis of BD in the future.

Keywords Brain death · DWI · MRI · Apparent diffusion coefficient values

Brain death (BD) is defined as the irreversible loss of all brain function, including brainstem function. Three essential findings in BD are coma, absence of brainstem reflexes, and apnea [1–5]. An evaluation for BD should be considered in patients who have suffered a massive, irreversible brain injury of identifiable cause. A patient determined to be brain dead is legally and clinically dead. The diagnosis of BD is primarily clinical and has been demonstrated using angiography or radiotracer methods. Magnetic resonance imaging (MRI) has been reported to demonstrate brain herniation and absent vascular flow [6–9]. Diffusion-weighted imaging (DWI) of the brain is establishing itself as a sensitive method for the detection of cerebral ischemic changes. The use of DWI to determine BD has been reported in only one case report. No study about this topic currently exists. The purpose of the present study was to determine the role of DWI and investigate the use of DWI in the diagnosis of BD.

Methods

Patients

The present study was approved by our ethics committees and it was performed according to the principles of the Declaration of Helsinki and institutional guidelines. All

H. Selcuk
Department of Radiology, Division of Neuroradiology,
Bakirkoy State Hospital,
KMP Istanbul 34300, Turkey

S. Albayram · Z. I. Hasiloglu · O. Kizilkilic · N. Kocer · C. Islak
Department of Radiology, Division of Neuroradiology,
Cerrahpasa Medical School,
KMP Istanbul 34300, Turkey

E. Tureci (✉)
Department of Anesthesiology, Cerrahpasa Medical School,
KMP Istanbul 34300, Turkey
e-mail: turecie@gmail.com

E. Cagil
Cerrahpasa Medical School,
KMP Istanbul 34300, Turkey

relatives of each BD patient and control subjects provided written informed consent before their enrollment in the study.

We prospectively evaluated 22 patients diagnosed with clinical BD from June 2007 to July 2010. The intensive care unit (ICU) referred 22 BD patients for evaluating MRI (9 women and 13 men; mean age, 39.63 ± 15.1 years; age range, 9–66 years). Initial causes of BD were head trauma ($n=7$), intracerebral hemorrhage ($n=2$), subarachnoid hemorrhage from an aneurysm rupture ($n=10$), anoxia with cardiac arrest ($n=2$), and an intracranial tumor ($n=1$).

Neurologic states that can mimic BD, including drug intoxication or poisoning, hypothermia, locked-in syndrome, and cases with bilateral cerebral hemisphere involvement, were excluded. All of the patients were evaluated with the Glasgow Coma Scale. The BD diagnosis was made according to criteria established by local law, including absence of eye opening, lack of spontaneous respiration, lack of spontaneous or evoked movement other than spinal cord reflex movements, absence of all brainstem reflexes, no return of neurologic function after a 6-h observation, and no spontaneous respiratory effort after an apnea challenge.

Since we designed this study in order to present the accuracy of diffusion imaging, we did not study other MR sequences. All clinical criteria for BD were present in all 22 patients before MRI, including a positive apnea test (duration, 10–15 min; 15-min preoxygenation with 100% oxygen; oxygenation catheter at the trachea level at a rate of 6 L/min; a partial pressure of carbon dioxide value of 60 mmHg or higher confirmed apnea). MRI was performed within the first 3 h after the decision of BD.

Control group patients were chosen from our hospital, had applied for knee MR examination, had no neurological problem, and were in the same age and gender group. Subjects in the control group were informed about the DWI application and they provided informed consent.

Imaging

All studies were performed using a Symphony imager (Siemens Medical Systems, Erlangen, Germany) operating at 1.5 T. A standard head coil with standard restraints was used to fix the subject's head position. In addition to axial DW images, conventional T1-weighted, T2-weighted, fluid-attenuated inversion recovery, and proton density-weighted images were obtained. Two neuroradiologists (H.S. and S.A.) evaluated all the images.

DWI was performed using a spin-echo echo-planar imaging sequence with a time to repetition/time to echo in spin of 4,000/103, a gradient strength of 25 mT/m, 5-mm thick sections, an intersection gap of 2.5 mm, a field of view of 230×230 mm², and a matrix size of 128×128 interpolated to 256×256 . Diffusion was measured in three orthogonal directions (x , y , and z) with two b values (0 and

1,000 s/mm²). The total acquisition time for the DW images was 30 s.

Data analysis

DW images belonging to the control and BD groups were transferred to a separate workstation for data analysis. First, the images in the three orthogonal directions were coregistered. The natural logarithms of the images were averaged to form a rotationally invariant resultant image. By using a linear least squares regression on a pixel-by-pixel basis, the resultant image and natural logarithm of the reference T2-weighted image ($b=0$) were fitted to the b values; the slope of the fitted line was the average apparent diffusion coefficient (ADC_{av}). Calculations were performed using a commercially available software program (Leonardo; Siemens Medical Solutions). We measured regions of interest (ROI) from one hemisphere (the left) because BD is a diffuse process. In the left hemisphere (right hemisphere in 3 cases because of left hemisphere pathology), 13 distinct neuroanatomic structures were selected for the analysis: frontal, parietal, temporal, occipital, and cerebellar gray matter and white matter; the putamen; the thalamus; and the pons (Fig. 1). Gray matter is more edematous in the brains of the BD patients. Therefore, it is easier to distinguish white and gray matter. We tried to distinguish gray and white matter when possible. The ROI were manually drawn on the ADC map images on which the structures could easily be identified. ROI measurement was repeated at least three times on every area, and the mean value was calculated for the control and BD groups. For each ROI, the mean, standard deviation, and range of the ADC_{av} values were obtained.

Statistical analysis

In this study, two neuroradiologist observers measured the ADC values separately, and based on their measurements, each came up with his/her diagnosis (as BD or not). Then, Cohen's kappa statistic is measured for this dichotomous classification by the observers.

We first provided a table of descriptive summary statistics (i.e., mean, median, standard deviation, and sample size (number of subjects)) of the variables for control and BD subjects, and then we tested the equality of their distributions using the Wilcoxon rank-sum test.

We also compared ADC values in white matter and gray matter of the same brain tissue (e.g., cerebellar of a BD patient or control subject). Hence, measurements are dependent because they are taken from the same subjects (e.g., white matter of cerebellar versus gray matter of cerebellum). Thus, we performed paired (or dependent) tests. We tested the equality of the distributions of ADC values in gray matter and white matter in each diagnostic group (i.e., in BD and healthy subjects) using the Wilcoxon signed-rank test.

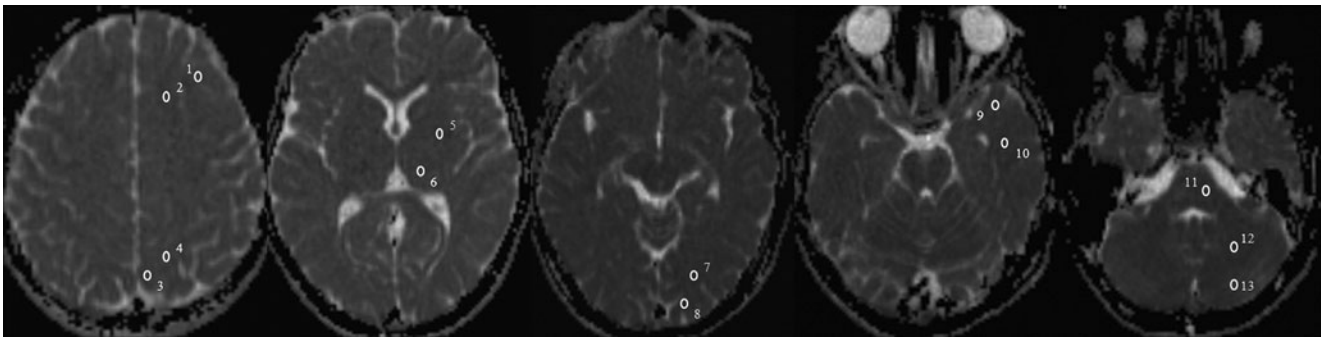


Fig. 1 ROI used in data analysis are superimposed on axial ADCav maps. 1 frontal gray matter, 2 frontal white matter, 3 parietal gray matter, 4 parietal white matter, 5 putamen, 6 thalamus, 7 occipital

white matter, 8 occipital gray matter, 9 temporal gray matter, 10 temporal white matter, 11 pons, 12 cerebellar white matter, 13 cerebellar gray matter

ADC values in white and gray matter of the cerebellum, parietal lobe, occipital lobe, temporal lobe, frontal lobe, pons, thalamus, and basal ganglion (BG) are related to the diagnosis condition (BD versus control) and determine threshold ADC values to classify a subject as BD or control.

Results

Since Cohen's interrater kappa values for the two neuro-radiologists was 0.95, the agreement is quite well. Then, we went on to use the measurements in our further analysis, which was conducted on the average ADC values measured by the two observers.

We tested the distributions of ADC values between male and female subjects separately for BD patients and healthy controls. We only report the significant results henceforth. ADC values for female BD patients were significantly greater than those for male BD patients ($p=0.0470$).

DWI showed diffuse hyperintense areas almost entirely covering both hemispheres, corresponding to diffuse edema (Fig. 2). Regional ADCav values are presented in Table 1. Additionally, in all cases, other MR images revealed diffuse sulcal effacement with hyperintense areas in both hemispheres, cerebellar tonsillar herniation, and no evidence of arterial flow in the intracranial circulation above the level of the supraclinoid portion of the internal carotid arteries (Figs. 3 and 4).

In the normal control group, the mean ADCav values were $(0.76\pm 0.03)\times 10^{-3}$ mm²/s for the frontal white matter, $(0.88\pm 0.05)\times 10^{-3}$ mm²/s for the frontal cortical gray matter, $(0.72\pm 0.03)\times 10^{-3}$ mm²/s for the temporal white matter, $(0.86\pm 0.04)\times 10^{-3}$ mm²/s for the temporal cortical gray matter, $(0.77\pm 0.04)\times 10^{-3}$ mm²/s for the parietal white matter, $(0.87\pm 0.04)\times 10^{-3}$ mm²/s for the parietal cortical gray matter, $(0.72\pm 0.03)\times 10^{-3}$ mm²/s for the occipital white matter, $(0.85\pm 0.04)\times 10^{-3}$ mm²/s for the occipital cortical gray matter, $(0.69\pm 0.03)\times 10^{-3}$ mm²/s for the cerebellar white matter, $(0.79\pm 0.06)\times 10^{-3}$ mm²/s for the cerebellar cortical gray matter, $(0.75\pm 0.03)\times 10^{-3}$ mm²/s

for the pons, $(0.76\pm 0.03)\times 10^{-3}$ mm²/s for the thalamus, and $(0.77\pm 0.03)\times 10^{-3}$ mm²/s for the putamen. ADC values for all locations in BD patients were significantly smaller than those in control subjects ($p<0.0001$; Table 2).

We compared the ADC values for gray matter versus white matter in BD patients and in healthy control groups. The ADC values for white matter in all neuroanatomic areas were significantly smaller than those for the gray matter in both BD patients and healthy control subjects ($p<0.0001$).

We examined the relationship between ADC values for white and gray matter of the cerebellum, parietal lobe, occipital lobe, temporal lobe, frontal lobe, pons, thalamus, and BG and the diagnosis condition (BD versus control) and assessed threshold ADC values required to classify a subject as BD or control (Table 3). The sensitivity, specificity, positive predictive value, negative predictive value, and correct classification rate of ADC cutoff values to distinguish BD from control groups were 100%. Importantly, we obtained perfect classification of brain dead and control subjects using ADC values for all locations.

Discussion

When a full clinical examination is conclusively performed, including assessments of both brainstem reflexes and the apnea test, no additional testing is required to determine BD. In some patients, skull or cervical injuries, cardiovascular instability, or other factors may make it impossible to complete parts of the assessment safely. Under such circumstances, a confirmatory test verifying BD is necessary [5]. In several European, Central and South American, and Asian countries, confirmatory testing is required by law. Certain countries (e.g., Sweden) require only cerebral angiography. In the US, the choice of tests is left to the discretion of the physician; however, bedside tests seem to be preferred [1]. Confirmatory tests for the determination of BD include electroencephalography (EEG), angiography, transcranial Doppler ultrasonography, and MRI [5].

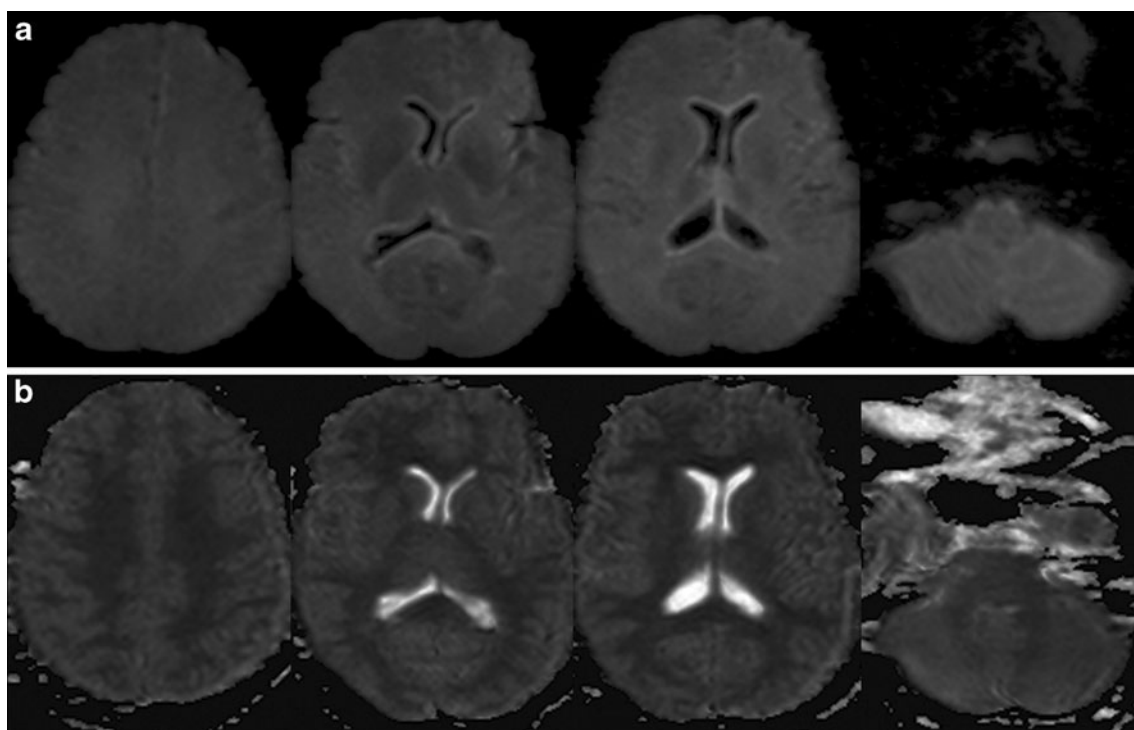


Fig. 2 Four sequential diffusion-weighted (**a**) and ADC map (**b**) images. DW images and ADC maps show diffuse hyperintense areas and decreased ADC values almost entirely covering both hemispheres,

corresponding to diffuse edema. Note that white matter involvement is more prominent than gray matter involvement

In EEG, BD is confirmed by documenting the absence of electrical activity during at least 30 min of recording that adheres to the minimal technical criteria for EEG recording in suspected BD as adopted by the American Electroencephalographic Society using 16-channel EEG instruments. However, setting the EEG machine at a high level of sensitivity may increase artifacts, which are abundant in the ICU because of the presence of multiple devices [10]. In transcranial Doppler ultrasonography, BD is confirmed by small systolic peaks in early systole without diastolic flow, or reverberating flow, indicating very high vascular resistance associated with greatly increased intracranial pressure. Because as many as 10% of patients may not have temporal insonation windows because of skull thickness, the initial absence of Doppler signals cannot be interpreted as being consistent with BD [3, 5, 11].

In angiography (conventional, computerized tomographic, magnetic resonance, and radionuclide), BD is confirmed by demonstrating the absence of intracerebral filling at the level of the carotid bifurcation or Circle of Willis. The external carotid circulation is patent, and filling of the superior sagittal sinus may be delayed [12]. Cerebral radionuclide angiography does not adequately image the vasculature of the posterior fossa [13]. The traditional gold standard has been four-vessel cerebral angiography. However, this technique has certain drawbacks that have limited its routine use: it is invasive, costly, and of limited availability because it requires

a neuroradiology room with expert staff [12, 14]. Cerebral arteriography is often difficult to perform in a critically ill, unstable patient. Additionally, repeated contrast injections may increase the risk of nephrotoxicity and decrease the acceptance rate in organ recipients. Therefore, new noninvasive radiological tests like MRI, magnetic resonance angiography (MRA), and computerized tomography angiography (CTA) have been proposed to replace catheter angiography. Studies on MRI and MRA dated back to 2002 [9, 15], but CTA has recently attracted attention. BD was first diagnosed with CTA by Dupas et al. [16]. The sensitivity and specificity was 100% in the study. Based on this publication, France and the Netherlands accepted CTA as a confirmatory test for BD diagnosis. However, the sensitivity and specificity have been lower in recent studies [17–20]. Although many of the methods evaluate blood flow, DWI shows neuronal damage fundamentally.

MRI has already been shown to demonstrate phenomena such as the absence of cerebral perfusion and increased enhancement of facial structures (e.g., the “hot nose sign”). Orrison et al. [6] have reported the MR criteria of BD to include transtentorial herniation and foramen magnum herniation, absent intracranial vascular flow voids, poor differentiation between gray and white matter, absent intracranial enhancement, carotid artery enhancement, and the hot nose sign. MR angiography does not display supraclinoid carotid arteries.

Table 1 The ADCav values in all locations

Case	Age	Sex	Causes	ADCav values												MRI findings			
				Frontal		Temporal		Parietal		Occipital		Cerebellum		Pons	Thalamus	Putamen	SE	CH	IO
				WM	GM	WM	GM	WM	GM	WM	GM	WM	GM						
1	47	M	Trauma	0.22±0.02	0.48±0.05	0.28±0.03	0.42±0.04	0.26±0.05	0.51±0.11	0.30±0.03	0.53±0.06	0.19±0.05	0.54±0.04	0.38±0.05	0.42±0.05	0.45±0.05	+	+	+
2	53	M	ICH	0.29±0.02	0.48±0.05	0.32±0.01	0.55±0.05	0.28±0.02	0.48±0.05	0.29±0.02	0.45±0.05	0.41±0.03	0.56±0.05	0.43±0.04	0.38±0.04	0.42±0.05	+	+	+
3	66	M	Anoxia	0.41±0.05	0.57±0.06	0.41±0.02	0.54±0.05	0.38±0.04	0.52±0.02	0.44±0.05	0.52±0.05	0.32±0.07	0.49±0.04	0.43±0.03	0.47±0.05	0.54±0.05	+	+	+
4	37	F	Trauma	0.26±0.03	0.52±0.07	0.43±0.05	0.59±0.07	0.28±0.06	0.55±0.06	0.40±0.04	0.62±0.06	0.35±0.05	0.56±0.08	0.42±0.05	0.45±0.05	0.50±0.04	+	+	+
5	50	M	SAH	0.32±0.05	0.55±0.12	0.29±0.04	0.44±0.03	0.33±0.04	0.44±0.02	0.27±0.03	0.47±0.05	0.33±0.04	0.44±0.04	0.42±0.04	0.49±0.05	0.41±0.03	+	+	+
6	38	F	SAH	0.28±0.05	0.51±0.05	0.34±0.05	0.47±0.06	0.25±0.02	0.48±0.05	0.43±0.04	0.54±0.07	0.37±0.04	0.51±0.05	0.44±0.03	0.47±0.06	0.45±0.05	+	+	+
7	41	F	ICH	0.27±0.04	0.52±0.11	0.39±0.05	0.55±0.04	0.29±0.05	0.45±0.03	0.26±0.02	0.56±0.05	0.48±0.05	0.62±0.07	0.50±0.05	0.45±0.03	0.49±0.06	+	+	+
8	18	M	Trauma	0.15±0.01	0.41±0.08	0.26±0.04	0.42±0.05	0.19±0.02	0.49±0.08	0.20±0.05	0.40±0.03	0.29±0.01	0.40±0.04	0.47±0.05	0.30±0.02	0.35±0.03	+	+	+
9	11	M	Tumor	0.31±0.05	0.47±0.05	0.32±0.03	0.38±0.02	0.30±0.06	0.43±0.02	0.27±0.04	0.40±0.04	0.27±0.02	0.38±0.05	0.35±0.02	0.42±0.05	0.49±0.05	+	+	+
10	20	F	Trauma	0.26±0.03	0.46±0.05	0.27±0.01	0.35±0.05	0.28±0.02	0.53±0.09	0.33±0.04	0.47±0.05	0.50±0.05	0.46±0.05	0.51±0.05	0.43±0.05	0.48±0.05	+	+	+
11	36	F	SAH	0.35±0.05	0.54±0.05	0.46±0.05	0.51±0.04	0.32±0.07	0.40±0.02	0.32±0.03	0.51±0.06	0.24±0.03	0.41±0.04	0.42±0.04	0.48±0.03	0.55±0.03	+	+	+
12	34	M	SAH	0.27±0.04	0.45±0.05	0.31±0.05	0.47±0.05	0.28±0.03	0.32±0.02	0.35±0.05	0.43±0.04	0.26±0.04	0.44±0.03	0.38±0.05	0.47±0.05	0.42±0.07	+	+	+
13	45	M	SAH	0.43±0.05	0.53±0.04	0.20±0.03	0.52±0.05	0.32±0.09	0.52±0.04	0.33±0.02	0.46±0.05	0.29±0.05	0.41±0.04	0.49±0.05	0.46±0.05	0.53±0.05	+	+	+
14	58	M	Trauma	0.36±0.03	0.63±0.08	0.34±0.04	0.59±0.08	0.25±0.02	0.46±0.05	0.38±0.05	0.38±0.03	0.27±0.03	0.46±0.05	0.43±0.04	0.42±0.05	0.46±0.05	+	+	+
15	44	F	SAH	0.38±0.05	0.62±0.05	0.35±0.05	0.54±0.05	0.38±0.05	0.40±0.02	0.38±0.05	0.49±0.05	0.53±0.07	0.63±0.06	0.46±0.05	0.50±0.04	0.42±0.05	+	+	+
16	55	F	SAH	0.41±0.04	0.51±0.03	0.36±0.05	0.48±0.05	0.34±0.03	0.38±0.05	0.42±0.04	0.51±0.05	0.44±0.06	0.55±0.05	0.48±0.05	0.53±0.05	0.43±0.03	+	+	+
17	38	M	SAH	0.28±0.02	0.45±0.04	0.33±0.04	0.50±0.07	0.26±0.02	0.43±0.04	0.30±0.03	0.48±0.08	0.37±0.05	0.59±0.05	0.52±0.05	0.49±0.04	0.45±0.05	+	+	+
18	45	M	SAH	0.23±0.03	0.38±0.07	0.36±0.02	0.48±0.10	0.24±0.05	0.50±0.02	0.38±0.06	0.55±0.07	0.18±0.05	0.31±0.03	0.31±0.02	0.42±0.11	0.44±0.04	+	+	+
19	53	M	Anoxia	0.18±0.04	0.40±0.02	0.28±0.04	0.44±0.06	0.25±0.02	0.48±0.05	0.28±0.04	0.46±0.05	0.35±0.07	0.50±0.06	0.48±0.04	0.39±0.04	0.39±0.03	+	+	+
20	9	F	Trauma	0.24±0.04	0.36±0.09	0.28±0.04	0.36±0.05	0.27±0.06	0.38±0.02	0.40±0.05	0.50±0.06	0.19±0.03	0.36±0.06	0.31±0.04	0.40±0.04	0.36±0.04	+	+	+
21	48	M	SAH	0.22±0.02	0.48±0.05	0.28±0.03	0.42±0.04	0.23±0.02	0.44±0.03	0.30±0.03	0.53±0.06	0.19±0.05	0.54±0.04	0.38±0.05	0.42±0.05	0.45±0.05	+	+	+
22	26	F	Trauma	0.20±0.05	0.32±0.06	0.15±0.01	0.32±0.06	0.18±0.03	0.34±0.02	0.32±0.07	0.38±0.05	0.27±0.04	0.42±0.04	0.40±0.04	0.42±0.06	0.45±0.10	+	+	+
				0.28±0.07	0.48±0.08	0.31±0.07	0.47±0.07	0.28±0.05	0.45±0.06	0.33±0.06	0.48±0.06	0.32±0.10	0.48±0.08	0.42±0.05	0.44±0.04	0.45±0.05			

WM white matter, GM gray matter, SE sulcal effacement, HN cerebellar herniation, IO internal carotid artery occlusion, ICH intracerebral hemorrhage, SAH subarachnoid hemorrhage

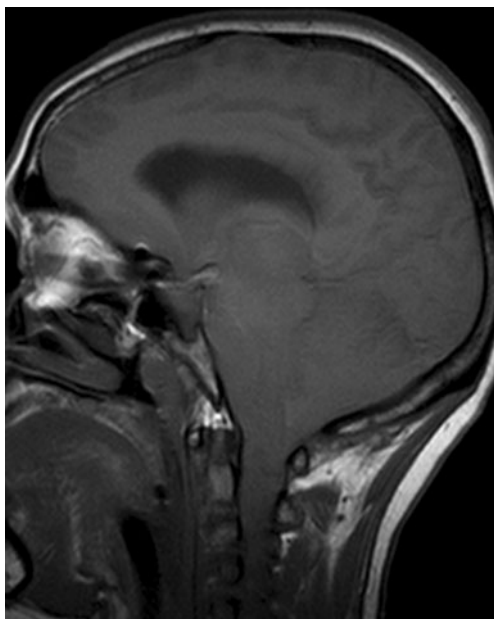


Fig. 3 T1-weighted fast spin-echo sagittal sequence shows the downward displacement of the diencephalon and brainstem with tonsillar herniation

Changes in the brain following BD occur as a function of time. The pathogenesis includes direct cellular injury potentiated by a vicious cycle from failure of blood flow, hypoxia, cerebral acidosis, and endothelial swelling to brain edema, herniation, and aseptic necrosis of the brain. Gross examination of such brain specimens shows a dusky, congested cerebral cortex, generalized brain swelling, a swollen pituitary gland, and macerated cerebellum. Microscopically, there is pan-necrosis of the nervous tissue and extensive foci of necrosis throughout the cerebrum, brainstem, and

Table 2 Mean ADCav values for BD in all the locations compared with mean ADCav values for controls groups

Location	BD	Normal	<i>p</i> values
Cerebellar WM	0.32±0.10	0.69±0.03	0.0001
Cerebellar GM	0.48±0.08	0.79±0.06	0.0001
Pons	0.42±0.05	0.75±0.03	0.0001
Parietal WM	0.28±0.05	0.77±0.04	0.0001
Parietal GM	0.45±0.06	0.87±0.04	0.0001
Occipital WM	0.33±0.06	0.72±0.03	0.0001
Occipital GM	0.48±0.06	0.85±0.04	0.0001
Temporal WM	0.31±0.07	0.72±0.03	0.0001
Temporal GM	0.47±0.07	0.86±0.04	0.0001
Frontal WM	0.28±0.07	0.76±0.03	0.0001
Frontal GM	0.48±0.08	0.88±0.05	0.0001
Thalamus	0.44±0.04	0.76±0.03	0.0001
Putamen	0.45±0.05	0.77±0.03	0.0001

cerebellum. Physiological changes following BD are so severe that progressive somatic deterioration and cardiac standstill will inevitably occur despite extensive life support. Several subsequent studies have suggested that BD does not always rapidly lead to somatic death [21].

During acute cerebral ischemia, the rapid failure of high-energy metabolism and associated ionic pumps leads to the migration of sodium and calcium into the cell. The subsequent influx of osmotically obligated water results in cellular swelling and a decrease in the extracellular volume fraction. Decreases in the ADC of brain water have been shown to coincide with the onset of acute cerebral edema, and this relationship allows for visualization of the extent of the ischemic territory as a hyperintense region in a DW image [22–26].

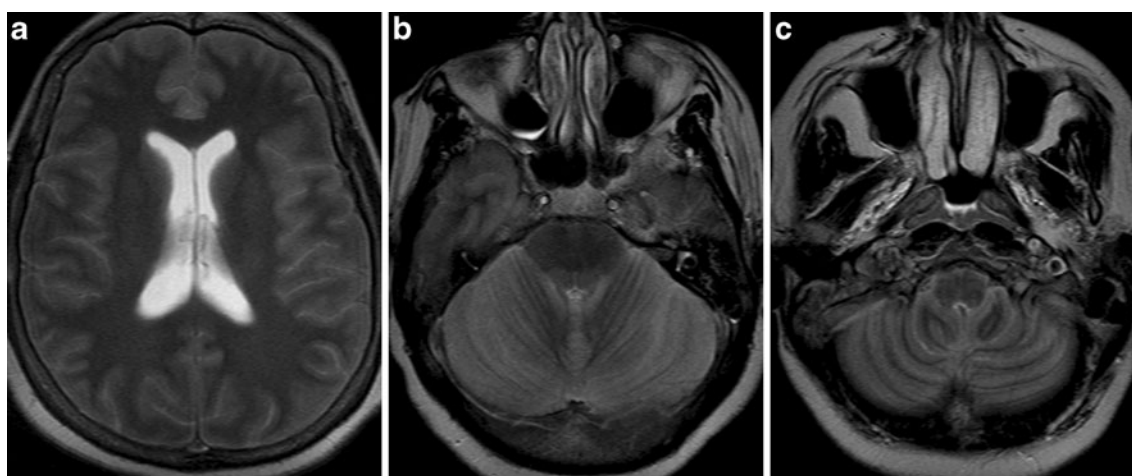


Fig. 4 a–c T2-weighted axial sequences show diffuse sulcal effacement with hyperintense areas in both hemispheres, cerebellar tonsillar herniation, and no evidence of arterial flow in the

intracranial circulation above the level of the supraclinoid portion of the internal carotid arteries

Table 3 The ranges (i.e., min and max) of ADC values and threshold values in all the location

Location	BD		Control groups		Threshold
	Min	Max	Min	Max	
Cerebellar WM	18	53	62	78	57.5
Cerebellar GM	31	63	72	88	67.5
Pons	31	52	65	80	58.5
Parietal WM	18	38	71	86	54.5
Parietal GM	32	55	80	98	67.5
Occipital WM	20	44	66	78	55
Occipital GM	38	62	78	98	70
Temporal WM	15	46	66	78	56
Temporal GM	32	59	78	98	68.5
Frontal WM	15	43	72	91	57.5
Frontal GM	32	62	76	102	69.5
Thalamus	30	53	70	83	61.5
BG	35	55	70	88	62.5

To our knowledge, no DWI study of BD has been previously reported. The only case report that has been published, by Lowblad and Bassetti [27], reported a decrease in the measured ADC values in the cerebral and cerebellar white and gray matter in a BD patient. We found a statistically significant decrease in ADC for all areas in patients compared with the control group. The decrease in ADC values was greater in white matter than in gray matter for both cerebral and the cerebellar hemispheres.

Well-documented differences exist in the neurochemical response to ischemia of white matter compared with gray matter compartments of the brain [28]. Differences in gray matter and white matter diffusion in stroke and/or BD could be due to variability between these two tissue types at any stage in the process that leads from ischemia to altered diffusion. Specifically, the observed diffusion contrast in gray matter and white matter could be caused by differences in the mismatch between the blood supply and metabolic demand, the type and/or severity of the histopathologic response to ischemic injury, or the mechanisms by which histopathologic changes lead to altered diffusion [29]. With regard to the histopathologic response, gray matter has been traditionally considered to be more vulnerable than white matter to early ischemia [30]. However, more recent findings in experimental models of stroke have demonstrated that ischemic damage to white matter occurs earlier and with greater severity than previously appreciated [31, 32]. With respect to the histopathologic–biophysical diffusion mechanisms, intracellular accumulation of water and enlargement of the periaxonal space were found in myelinated fiber tracts in animal models, with differences

in the dependence of ischemic gray matter and white matter diffusion on total water accumulation [31, 32]. A significant difference in ADC values of white and gray matter in our study may be explained by the above-mentioned studies. Although we measured white and gray matter separately, ADC measures of gray or white matter can be used to differentiate BD because the upper range of gray matter values in BD patients was smaller than the lower range of white matter ADC values in controls.

Oppenheim et al. [33] examined the relationship between infarction and ADC values of the tissue. They reported that the sensitivity and specificity of ADC and the quantitative perfusion cutoff values to distinguish the final infarct from the oligemic area were high. The ADC cutoff value was $0.74 \times 10^{-3} \text{ mm}^2/\text{s}$, the specificity was 95%, and the sensitivity was 83%. However, Arakawa et al. [34] defined threshold values for stroke in a study in which they included 21 patients within the first 24 h of ischemic stroke. They also revealed that ADC, cerebral blood volume, and cerebral blood flow threshold values in white matter were lower than in gray matter. In the current study, we also searched for a cutoff ADC value that might support BD and we detected cutoff values for both white and gray matter. The sensitivity, specificity, positive and negative predictive values, and correct classification rate of ADC cutoff values to distinguish BD from control groups were 100%. Cutoff ADC values were reported to distinguish between ischemia and infarction in some studies, but they were not previously studied for BD. We have mainly planned to measure DWI and ADC values. We have not considered comparing it with MRI. A cutoff value has been found. However, this value may be different for the other MRI scanners and DWI protocols. Therefore, hospitals have to determine a cutoff value for their own scanners and protocols, based on values in normal controls. In addition, although there is the difference in ADC values between female and male BD patients, this difference does not have a clinical consequence.

Although MRI is noninvasive and fast in determining BD, some difficulties exist. Because BD patients are ventilated and monitored in the ICU, transporting these patients is challenging. Additionally, MRI-compatible ventilators and monitors are mandatory for performing DWI. Technical difficulty may occur because of magnet incompatibility with lines, ventilator tubes, and other hardware. However, diffusion MRI may be preferred because it is fast and noninvasive, compared with cerebral angiography.

Consequently, confirmatory tests and investigations are needed in specific situations and in cases of a difficult diagnosis, although BD is a clinical diagnosis. DWI might be preferred because it is noninvasive, can be performed quickly (in only 30 s), and is also an alternative method supporting diagnosis using direct quantitative values. In the current study, cutoff values were obtained for BD diagnosis.

Conflict of interest We declare that we have no conflict of interest.

References

- Wijdicks EF (2001) The diagnosis of brain death. *N Engl J Med* 344:1215–1221
- Wijdicks EFM (2001) Clinical diagnosis and confirmatory testing of brain death in adults. In: Wijdicks EFM (ed) *Brain death*. Lippincott William & Wilkins, Philadelphia, pp 61–90
- Wijdicks EF (1995) Determining brain death in adults. *Neurology* 45:1003–1011
- Report of the Quality Standards Subcommittee of the American Academy of Neurology (1995) Practice parameters for determining brain death in adults. *Neurology* 45:1012–1014
- Wijdicks EF, Varelas PN, Gronseth GS, Greer DM, American Academy of Neurology (2010) Evidence-based guideline update: determining brain death in adults: report of the Quality Standards Subcommittee of the American Academy of Neurology. *Neurology* 74:1911–1918
- Orrison WW, Champlin AM, Kesterson OL et al (1994) MR “hot nose sign” and “intravascular enhancement sign” in brain death. *AJNR Am J Neuroradiol* 15:913–916
- Feldmann E, Gandy SE, Becker R et al (1988) MRI demonstrates descending transtentorial herniation. *Neurology* 38:697–701
- Jones KM, Barnes PD (1992) MR diagnosis of brain death. *AJNR Am J Neuroradiol* 13:65–66
- Ishii K, Onuma T, Kinoshita T et al (1996) Brain death: MR and MR angiography. *AJNR Am J Neuroradiol* 17:731–735
- American Electroencephalographic Society (1994) Guideline three: minimum technical standards for EEG recording in suspected cerebral death. *J Clin Neurophysiol* 11:10–13
- Petty GW, Mohr JP, Pedley TA et al (1990) The role of transcranial Doppler in confirming brain death: sensitivity, specificity, and suggestions for performance and interpretation. *Neurology* 40:300–303
- Bradac GB, Simon RS (1974) Angiography in brain death. *Neuroradiology* 7:25–28
- Donohue KJ, Frey KA, Gerbaudo VH et al (2003) Society of nuclear medicine procedure guideline for brain death scintigraphy. *J Nucl Med* 44:846–851
- Nau R, Prange HW KJ, Kukowski B, Sander D, Tchorsch R, Rittmeyer K (1992) Results of four technical investigations in fifty clinically brain dead patients. *Intensive Care Med* 18:82–88
- Karantanas AH, Hadjigeorgiou GM, Paterakis K, Sfiras D, Komnos A (2002) Contribution of MRI and MR angiography in early diagnosis of brain death. *Eur Radiol* 12:2710–2716
- Dupas B, Gayet-Delacroix M, Villers D, Antonioli D, Veccherini MF, Soullou JP (1998) Diagnosis of brain death using two-phase spiral CT. *AJNR Am J Neuroradiol* 19:641–647
- Leclerc X, Taschner CA, Vidal A, Strecker G, Savage J, Gauvrit JY, Pruvot JP (2006) The role of spiral CT for the assessment of the intracranial circulation in suspected brain death. *J Neuroradiol* 33:90–95
- Frampas E, Videcoq M, de Kerviler E, Ricolfi F, Kuoch V, Mourey F, Tenaillon A, Dupas B (2009) CT angiography for brain death diagnosis. *AJNR Am J Neuroradiol* 30:1566–1570
- Van der Lugt A (2010) Imaging tests in determination of brain death. *Neuroradiology* 52:945–947
- Gutierrez LG, Rovira A, Portela LA, Leite Cda C, Lucato LT (2010) CT and MR in non-neonatal hypoxic–ischemic encephalopathy: radiological findings with pathophysiological correlations. *Neuroradiology* 52:949–976
- Wijdicks EF, Pfeifer EA (2008) Neuropathology of brain death in the modern transplant era. *Neurology* 70:1234–1237
- Klatzo I (1987) Pathophysiological aspects of brain edema. *Acta Neuropathol* 72:236–239
- Davis D, Ulatowski J, Eleff S et al (1994) Rapid monitoring of changes in water diffusion coefficients during reversible ischemia in cat and rat brain. *Magn Reson Med* 31:454–460
- Mintorovitch J, Moseley ME, Chileuit L et al (1991) Comparison of diffusion- and T2-weighted MRI for the early detection of cerebral ischemia and reperfusion in rats. *Magn Reson Med* 18:39–50
- Minematsu K, Li L, Fisher M et al (1992) Diffusion-weighted magnetic resonance imaging: rapid and quantitative detection of focal brain ischemia. *Neurology* 42:235–240
- Sotak CH (2002) The role of diffusion tensor imaging in the evaluation of ischemic brain injury—a review. *NMR Biomed* 15:561–569
- Lövblad KO, Bassetti C (2000) Diffusion-weighted magnetic resonance imaging in brain death. *Stroke* 31:539–542
- Dohmen C, Kumura E, Rosner G et al (2001) Adenosine in relation to calcium homeostasis: comparison between gray and white matter ischemia. *J Cereb Blood Flow Metab* 21:503–510
- Mukherjee P, Bahn MM, McKinstry RC et al (2000) Differences between gray matter and white matter water diffusion in stroke: diffusion-tensor MR imaging in 12 patients. *Radiology* 215:211–220
- Marcoux FW, Morawetz RB, Crowell RM et al (1982) Differential regional vulnerability in transient focal cerebral ischemia. *Stroke* 13:339–346
- Pantoni L, Garcia JH, Gutierrez JA (1996) Cerebral white matter is highly vulnerable to ischemia. *Stroke* 27:1641–1647
- Kuroiwa T, Nagaoka T, Ueki M et al (1998) Different apparent diffusion coefficient: water content correlations of gray and white matter during early ischemia. *Stroke* 29:859–865
- Oppenheim C, Grandin C, Samson Y et al (2001) Is there an apparent diffusion coefficient threshold in predicting tissue viability in hyperacute stroke? *Stroke* 32:2486–2491
- Arakawa S, Wright PM, Koga M et al (2006) Ischemic thresholds for gray and white matter: a diffusion and perfusion magnetic resonance study. *Stroke* 37:1211–1216